Journal of Mechatronics and Robotics

Original Research Paper

Design and Development of a Quarter-Car Model Active Suspension System for a Mobile Robot to Enhance Terrain Adaptability with Better Stability and Mobility

Rukshan Gamage, Chamod Rathnayake, Ruwan Kalubowila and Sanjaya Thilakarathne

Department of Instrumentation and Automation Technology, University of Colombo, Homagama, Sri Lanka

Article history
Received: 22-08-2024
Revised: 30-09-2024
Accepted: 08-10-2024

Corresponding Author:
Sanjaya Thilakarathne
Department of Instrumentation and Automation Technology, University of Colombo, Homagama, Sri Lanka
Email: sanjaya@iat.cmb.ac.lk

Abstract: Robotics is a field that represents an important milestone in modern technology. In this robotic field, new designs and solutions emerge daily and the service provided is immense. Among them, mobile robots are regarded as exceptional inventions. The ability to recognize and avoid obstacles is built into many mobile robots. However, the development of mobile robots that can recognize and navigate obstacles has received very little attention. In this study, a novel solution is introduced to fill this vacuum. This study aims to design and develop an active suspension system for a mobile robot, which would help robots move forward, overcome obstacles, and increase stability as well as mobility. The active suspension system of the robot is evaluated both practically and theoretically using different angled surfaces between 10 and 60 degrees. Additionally, the responses from the gyro and accelerometer sensors were examined for various terrain conditions. Through this study, both obstacle identification and wheel speed adjustment based on acquired data were aided when necessary to reduce the speed by 30-40%. The unique feature of this robot is its constant effort to stay horizontal and overcome rolling and bending. Additionally, introducing this novel solution can address significant issues, including the complexity of the control systems, the rise in production costs, and the intricate design of the existing robot suspension system.

Keywords: Active Suspension System, Linear Actuator, Mobile Robots, Quarter-Car Model

Introduction

One significant technological turning point in recent years is robotics. The robotics sector is developing quickly to meet the market's demands, people's everyday requirements, production, research initiatives, academic institutions, etc. The practical definition of robotics is the study, creation, and application of robot systems in industry (Sucuoğlu *et al*., 2016). Typically, harmful, dangerous, extremely repetitive and unpleasant jobs are performed by robots Elfasakhany *et al*. (2011). Furthermore, a growing number of technical studies and research projects include different types of robots (Sucuoğlu *et al*., 2016; Elfasakhany *et al*., 2011).

Mobile robots are among the most prevalent robotic types when discussing robotic types (Sucuoğlu *et al*., 2016). A mobile robot is a sophisticated mechatronics system that combines embedded control systems and mechanics to create transdisciplinary solutions and techniques (Oftadeh *et al*., 2013). In particular, a mobile robot can move indefinitely to fulfill its objective (Sucuoğlu *et al*., 2016). Generally, the application of mobile robots such as navigation, map creation, and self-position estimation is crucial (Zunaidi *et al*., 2006). Furthermore, it has long been the goal of many robotics experts to create mobile robots that can go anywhere they need to go (Datar *et al*., 2024). Preparing the working conditions and assumed features, such as the ability to move and apply flexibility in unstructured terrain, reducing uncontrollably high vertical motions and vibrations, and providing support, is the first step in developing a solution for the design of a mobile platform. Selecting the right suspension design is a crucial step in creating a wheeled robot that can navigate uneven terrain with efficient movement (Datar *et al*., 2024; Olinski and Cholewa, 2014).

A mobile robot's stability and mobility are greatly influenced by its suspension system. According to the

degree of control over suspension characteristics, suspension systems can be broadly classified as independent or dependent, active, passive, or semiactive (Olinski and Cholewa, 2014). A system that uses motors and electronics to adjust suspension stiffness and damping in real-time is known as an active suspension (Olinski and Cholewa, 2014; Attia, 2018). The height of the suspension is adjusted by the active suspension element, which enables the robot to adapt to the surface. The robot can be raised and lowered, the chassis can be leveled against gravity, the roll and pitch attitude can be adjusted for docking operations and the force can be evenly distributed across the wheels during low-speed operations thanks to the active suspension system (Datar *et al*., 2024; Olinski and Cholewa, 2014; Attia, 2018).

The aforementioned information served as the foundation for the researchers' efforts to develop and construct various active suspension systems for mobile robots, which would help robots move forward, overcome obstacles, and increase stability as well as mobility (Sujiwa and Suhadata, 2023; Yildiz *et al*., 2013). The key issues with those designs are the control systems' complexity, the production cost increase, and their intricate structure. In this study, a novel solution is introduced to overcome these problems which is a cost-effective simple framework with an active suspension system for helping robots move forward, overcome obstacles, and increase stability as well as mobility.

Literature Survey

Rather than building robots that traverse barriers head-on, much study has gone into creating robots that utilize sensors to identify and avoid obstacles. This section includes a summary of the literature on some of the studies most similar to the research conducted.

NASA was the organization that designed and oversaw a first-generation active suspension system. An overview of the requirements and advantages of active suspensions for crew mobility systems on the lunar surface is provided in this research (Bluethmann *et al*., 2010). This robot can be raised or lowered, the roll and pitch attitude can be changed for docking operations, the chassis can be leveled against gravity and the force can be distributed evenly across the six wheels while the robot is operating at a low speed. Apart from the current setup, the preliminary outcomes of a gradual redesign were examined and prospective ideas for lunar surface suspension systems were explained (Bluethmann *et al*., 2010; Zheng *et al*., 2018; Li *et al*., 2024; Dogruer, 2019).

Improving the mobility of vehicles in uneven terrain was illustrated by another research. This study provides insights into the mechanical construction requirements of the robot or vehicle by explicitly developing the criterion for the mobility of a wheeled vehicle in any terrain (Pan *et al*., 2023). To achieve better rough terrain mobility, the vehicle construction with an actively articulated suspension was discovered by this study. The crucial component in determining the surface's traversability was determined by analyzing the contact forces between the vehicle and the terrain (Pan *et al*., 2023). This design offers a way to improve mobility in tough terrain by utilizing the dynamics of the main body, which was different from many other similar designs (Zunaidi *et al*., 2006; Pan *et al*., 2023; Unluturk and Aydogdu, 2017).

A unique reconfigurable wheeled robot for off-road applications has been the subject of some research and development. In one study, the reconfigurable wheeled robot TIGER is designed, modeled, analyzed, and controlled using an elastic actuated mechanism that modifies the robot's pitch angles, ground clearance, and body roll to increase its dynamic stability on uneven terrain (Attia, 2018). Utilizing physical models of the rover and terrain, a second study compelled the development of strategies for enhancing mobile robot mobility in hazardous, uneven terrain (Chetan *et al*., 2017; Romsai and Nawikavatan, 2019). The construction of a wheeled movable platform that could traverse difficult terrain and was specifically meant to assist agricultural labor was the subject of another study (Olinski and Cholewa, 2014). Finally, unique reconfigurable wheeled robots were developed for off-road applications by these studies (Olinski and Cholewa, 2014; Attia, 2018; Romsai and Nawikavatan, 2019).

The development of an autonomous mobile robot with four-wheel drive and differential locomotion was discussed by the research of Crenganis *et al*. (2021). The capacity to move various kinds of freight through industrial areas and over uneven terrain was the primary purpose behind the development of this kind of mobile platform. A design similar to this was created by Hua *et al*. (2016). A mobile robot platform with four separate driving and steering wheels was represented by this robot. The mobile robot on wheels was outfitted with a visible camera and a thermal imager (Hua *et al*., 2016). The control of robotic cars in tough terrain with actively articulated suspensions was created by Paul Schenker *et al*. In this study, a wheel-terrain contact angle estimation technique was created using basic onboard sensors (Dogruer, 2019). The development of mobile robots with various suspension systems was the foundation of these literary works (Sucuoğlu *et al*., 2016; Crenganis *et al*., 2021; Hua *et al*., 2016; Dogruer, 2019; Ni *et al*., 2020).

A low-cost autonomous mobile robot was developed by Kasun and Ravinda. In this study, image processing and infrared sensor circuits were used to successfully lead

a robot down a path in an innovative and low-cost manner (Jinasena and Meegama, 2016). In 2026, Long-range control based on nrf24l01 was used by Sujiwa and Suhadata (2023) to develop and build a self-balancing robot. The MPU6050 sensor was utilized to determine the state of the robot's operation, which was managed by the remote control to measure the robot's tilt angle (Sujiwa and Suhadata, 2023, 2023). Cost-effective mobile robots were the main focus of these approaches (Elfasakhany *et al*., 2011; Sujiwa and Suhadata, 2023, 2023; Jinasena and Meegama, 2016; Pei and Kleeman, 2016; (Bledt *et al*., 2018).

A study on motion control of a ball screw system driven by a Permanent Magnet Stepper Motor (PMSM) was presented by John Cloutier. A servo system was created to enable operations at those velocities as this investigation revealed that it was challenging to use a PMSM for high-speed applications to function in feedforward mode (Cloutier, 2014). A few unique inventions that were similar to this mechanism have been found (Dave *et al*., 2014), (Fotuhi *et al*., 2022), (Badrinarayanan *et al*., 2018). These include the design, development, and study of remote-controlled screw jacks for four-wheel drive vehicles (Dave *et al*., 2014), the design and development of an industrial electromechanical cylinder driven by an electrical motor and ball screw (Fotuhi *et al*., 2022) and the development of an electro-mechanical linear actuator that uses roller screws (Badrinarayanan *et al*., 2018; Mallikarathne *et al*., 2023).

Materials and Methods

Design and Development of Active Suspension System

The primary component of this mobile robot is the active suspension system, which was initially designed and built. The conceptual model of our active suspension system can be seen in Fig. (1).

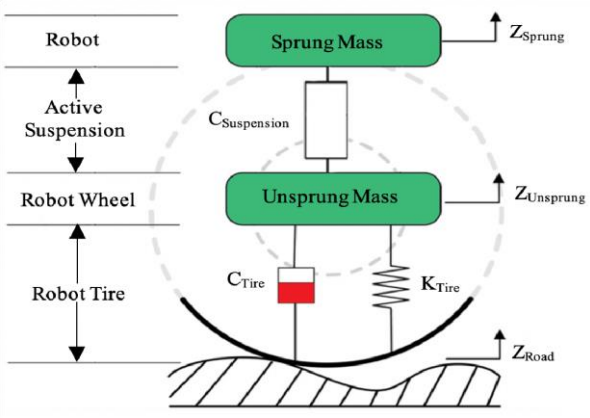

Fig. 1: The conceptual model of the active suspension system

The road displacement input and the displacement of the sprung and unsprung masses are represented by the variables ZRoad (ZR), ZSprung (ZS), and ZUnsprung (ZU), respectively. In addition, the tire's compressibility, damping, and stiffness of the suspension system are indicated by the symbols K_{Tire} (K_T), C_{Tire} (C_T), and $C_{Suspension}$ (C_S) respectively. The active suspension system is implemented between Sprung Mass (m_S) and Unsprung Mass (m_U), as shown in the above image.

The equations of motion for this mobile robot's quarter-car model active suspension system may be derived using Newton's laws and are represented as Eqs. (1-2) for Sprung (m_S) and Unsprung Masses (m_U):

$$m_s\ddot{Z}_s = C_s(\dot{Z}_U - \dot{Z}_s) \quad (1)$$

$$m_U\ddot{Z}_U = K_T(Z_R - Z_U) + C_T(\dot{Z}_R - \dot{Z}_U) - (m_S\ddot{Z})$$

$$m_U\ddot{Z}_U = K_T(Z_R - Z_U) + C_T(\dot{Z}_R - \dot{Z}_U) - C_S(\dot{Z}_U - \dot{Z}_S) \quad (2)$$

Where $\ddot{Z}_s$ is the acceleration of the sprung mass, $\dot{Z}_U$ and $\dot{Z}_S$ are the velocities of the unsprung and sprung mass, respectively. $\ddot{Z}_U$ is the acceleration of the unsprung mass and $\dot{Z}_R$ is the velocity of the road surface.

The linear representation of our dynamic suspension system in state-space form can be written as Eq. (3).

$$\dot{x} = Ax + Bu \quad (3)$$

The road input, which includes the road surface's displacement and velocity, is represented by the *u*, and the state vector is represented by *x*. Let the state variables x_1, x_2, x_3, and x_4 be equal to Z_S, $\dot{Z}_S$, Z_U, and $\dot{Z}_U$, respectively. Then, the state vector (*x*) and input vector (*u*) of this system are:

$$x = \begin{bmatrix} x_1 \\ x_2 \\ x_3 \\ x_4 \end{bmatrix}$$

$$u = \begin{bmatrix} Z_R \\ \dot{Z}_R \end{bmatrix}$$

The new Eqs. (4-5) can be obtained by replacing the state variables in Eqs. (1-2):

$$m_s\dot{x}_1 = C_S(x_4 - x_2) \quad (4)$$

$$m_U\dot{x}_3 = K_T(Z_R - x_3) + C_T(\dot{Z}_R - x_4) - C_S(x_4 - x_2) \quad (5)$$

Since $\dot{x}_1 = \dot{x}_2$ and $\dot{x}_3 = \dot{x}_4$, it is possible to derive Eqs. (6-7):

$$\dot{x}_1 = \dot{x}_2 = \frac{C_S}{m_s}(x_4 - x_2) \quad (6)$$

$$\dot{x}_3 = \dot{x}_4 = \frac{K_T}{m_U}(ZR - x_3) + \frac{C_T}{m_U}(\dot{Z}_R - x_4) - \frac{C_S}{m_U}(x_4 - x_2) \quad (7)$$

The dynamics of each state variable can be determined and the *A* and *B* matrices can be extracted as follows:

$$A = \begin{bmatrix} 0 & 1 & 0 & 0 \\ 0 & -\frac{C_S}{m_S} & 0 & \frac{C_S}{m_S} \\ 0 & 0 & 0 & 1 \\ 0 & \frac{C_S}{m_U} & -\frac{K_T}{m_u} & -\frac{C_T + C_S}{m_U} \end{bmatrix} B = \begin{bmatrix} 0 & 0 \\ 0 & 0 \\ 0 & 0 \\ \frac{K_T}{m_u m_U} & \frac{C_T}{m_u m_U} \end{bmatrix}$$

Consequently, the state-space representation of our dynamic suspension system can be seen below:

$$\begin{bmatrix} \dot{x}_1 \\ \dot{x}_2 \\ \dot{x}_3 \\ \dot{x}_4 \end{bmatrix} = \begin{bmatrix} 0 & 1 & 0 & 0 \\ 0 & -\frac{C_S}{m_S} & 0 & \frac{C_S}{m_S} \\ 0 & 0 & 0 & 1 \\ 0 & \frac{C_S}{m_U} & -\frac{K_T}{m_u} & -\frac{C_T + C_S}{m_U} \end{bmatrix} \begin{bmatrix} x_1 \\ x_2 \\ x_3 \\ x_4 \end{bmatrix} + \begin{bmatrix} 0 & 0 \\ 0 & 0 \\ 0 & 0 \\ \frac{K_T}{m_u m_U} & \frac{C_T}{m_u m_U} \end{bmatrix} \begin{bmatrix} Z_R \\ \dot{Z}_R \end{bmatrix}$$

$$\dot{x} \begin{bmatrix} 0 & 1 & 0 & 0 \\ 0 & -\frac{C_S}{m_S} & 0 & \frac{C_S}{m_S} \\ 0 & 0 & 0 & 1 \\ 0 & \frac{C_S}{m_U} & -\frac{K_T}{m_u} & -\frac{C_T + C_S}{m_U} \end{bmatrix} x + \begin{bmatrix} 0 & 0 \\ 0 & 0 \\ 0 & 0 \\ \frac{K_T}{m_u m_U} & \frac{C_T}{m_u m_U} \end{bmatrix} u$$

The output equation of our dynamic suspension system in state-space form can be written as Eq. (8):

$$y = Cx \tag{8}$$

where, *y* and *C* are the output vector and output matrix, respectively, and *x* is the state vector, as mentioned before:

$$y = \begin{bmatrix} x_1 \\ x_3 \end{bmatrix} = \begin{bmatrix} Z_S \\ Z_U \end{bmatrix}$$

The output matrix *C* can be extracted as follows:

$$C = \begin{bmatrix} 1 & 0 & 0 & 0 \\ 0 & 0 & 1 & 0 \end{bmatrix}$$

Consequently, the output equation for our dynamic suspension system can be seen below:

$$\begin{bmatrix} x_1 \\ x_3 \end{bmatrix} = \begin{bmatrix} Z_S \\ Z_U \end{bmatrix} = \begin{bmatrix} 1 & 0 & 0 & 0 \\ 0 & 0 & 1 & 0 \end{bmatrix} \begin{bmatrix} x_1 \\ x_2 \\ x_3 \\ x_4 \end{bmatrix}$$

$$y = \begin{bmatrix} 1 & 0 & 0 & 0 \\ 0 & 0 & 1 & 0 \end{bmatrix} x$$

The screw mechanism was used in the construction of this active suspension system which was worked as a linear actuator. SOLIDWORKS software was first used to design the suspension as shown in Fig. (2).

In this design, a pair of tubular shapes were employed, with one used for internal movement within the other. The motor was rigidly connected to the outer cylindrical tube as shown in Fig. (3). The shaft of the DC motor was linked to the screw shaft with a gear system of 1:48 ratio. The inner tube was attached to the nut. This assembly is slid on top of one another with a screw mechanism to maintain a vertical movement.

The suspension height is varied by a screw that is connected to a gear motor placed vertically. A single rotation of this motor causes the screw to move up or down a displacement of 1.5 mm. Hence, for every rotation of the screw, the robot moves 1.5 mm vertically. The maximum operating speed of the two-gear motors is 200 (±10%) RPM according to the specifications of the motor. The road angle has an impact on the robot's speed along the incline because, although the vertical speed (height adjustment) stays constant, the robot must travel a varied horizontal distance depending on the incline angle. The theoretical values of the maximum speed that driven motors may achieve to overcome barriers at various angles were determined by considering these parameters.

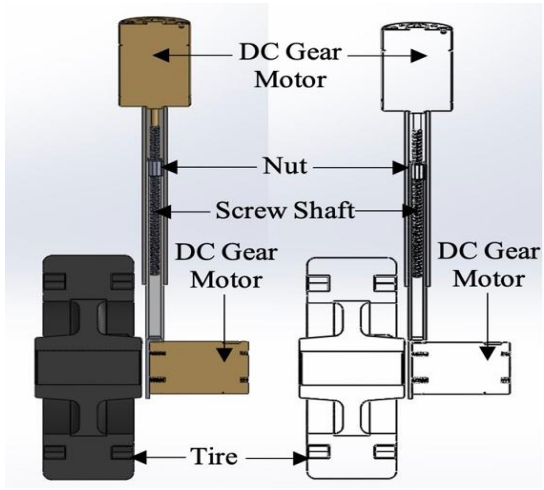

Fig. 2: The design of the active suspension system

Fig. 3: The formation of the active suspension system. (Quarter-vehicle model)

DOI: 10.3844/jmrsp.2024.39.48

The vertical speed can be determined by the screw motor's RPM and the movement per screw rotation with Eq. (9):

$$Vertical\ Speed = \frac{Screw\ Movement\ per\ Rotation \times RPM}{60} \quad (9)$$

$$Vertical\ Speed = \frac{0.0015m \times 200\ rev/\min}{60} = 0.005ms^{-1}$$

This indicates that at all inclination angles, the robot's vertical speed remains constant at 0.005ms^{-1}.

Considering the relationship between vertical speed and vehicle speed, the speed along the road or robot speed changes depending on the road's incline angle (θ), which can be seen in Eq. 10:

$$Robot\ Speed = \frac{Vertical\ Speed}{\sin\theta} \quad (10)$$

The maximum robot speed was calculated for different incline angles from 10^0-60^0 using Eq. 10:

$$Robot\ Speed\ for\ 10^0\ Angle = \frac{0.005ms^{-1}}{\sin 10^0} = 0.0288ms^{-1}$$

$$Robot\ Speed\ for\ 20^0\ Angle = \frac{0.005ms^{-1}}{\sin 20^0} = 0.01462ms^{-1}$$

$$Robot\ Speed\ for\ 30^0\ Angle = \frac{0.005ms^{-1}}{\sin 30^0} = 0.01ms^{-1}$$

$$Robot\ Speed\ for\ 40^0\ Angle = \frac{0.005ms^{-1}}{\sin 40^0} = 0.00778ms^{-1}$$

$$Robot\ Speed\ for\ 45^0\ Angle = \frac{0.005ms^{-1}}{\sin 45^0} = 0.00707ms^{-1}$$

$$Robot\ Speed\ for\ 50^0\ Angle = \frac{0.005ms^{-1}}{\sin 50^0} = 0.00653ms^{-1}$$

$$Robot\ Speed\ for\ 60^0\ Angle = \frac{0.005ms^{-1}}{\sin 60^0} = 0.00577ms^{-1}$$

The power required by a single motor in the robot chassis during startup was calculated using these velocities.

Design and Development of the Four-Wheel Robot

A four-wheel robot was designed using this quartervehicle model of the active suspension technology. The suspension system of this designed robot was driven by four DC gear motors, while the robot wheels were independently driven by an additional four motors. The designed robot with the active suspension system can be seen in Fig. (4).

When this designed robot was formed, two accelerometers were used to detect the change in the angle of the bed or chassis due to the uneven condition of the terrain. A control system was used to control each linear actuator or suspension according to the changing parameters of the accelerometers. The functional block diagram for the rover controller system or suspensions can be seen in Fig. (5).

In this diagram, disturbance 1 means noises generated by the accelerometer and the gyro sensor. Additionally, noises generated by motors and the heat of electronic devices are also taken under this. The friction of lead screws and heat generated due to friction of the lead screw is indicated by disturbance 2. Disturbances 1 and 2 were considered individually in motion control. The control system can be developed using the flow chart in Fig. (6).

In this flow chart, four motor controllers and an Arduino Mega Board were powered up using a 6 V (2850 mAh) battery. The linear actuator or suspension motor and robot wheel motor were controlled using each motor controller. Two accelerometers with gyros sensors were placed on the front and back of the robot body. The circuit diagram of the mobile robot can be seen in Fig. (7).

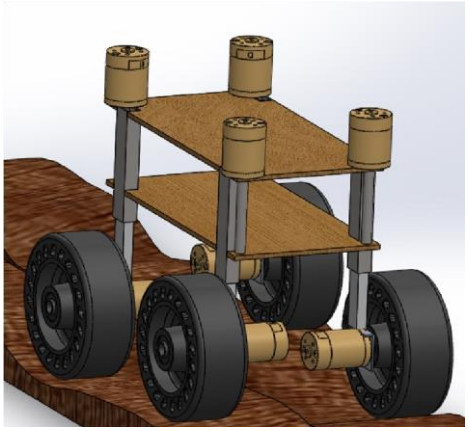

Fig. 4: The design of the mobile robot with the active suspension system

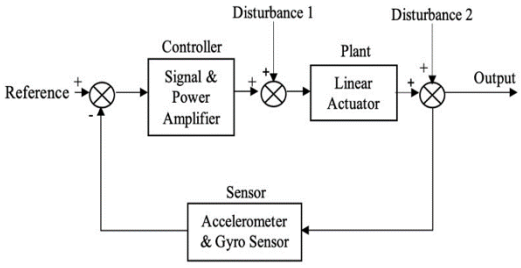

Fig. 5: The functional block diagram for the rover controller system or suspensions

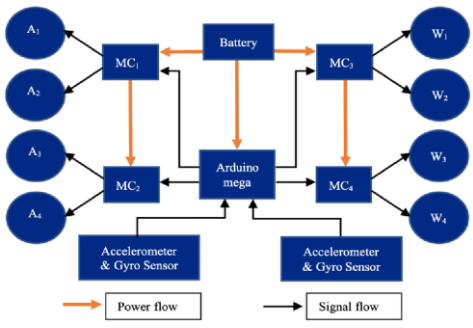

Fig. 6: The control system of the robot

DOI: 10.3844/jmrsp.2024.39.48

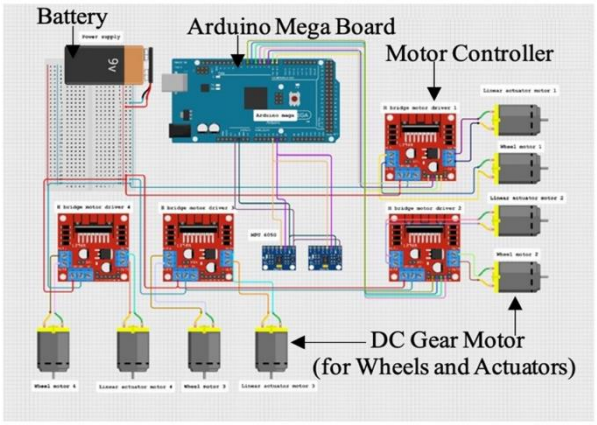

Fig. 7: The circuit diagram of the mobile robot

Given that the four motors powering the robot wheels vary in inclination degree, it is crucial to determine the power needed for each motor under various load scenarios. Eq. (11) can be used to determine the component of gravitational force acting parallel to the inclination:

$$F_x = mg\sin\theta \tag{11}$$

Similarly, Eq. (12) can be used to compute the normal force, which is the component of gravitational force perpendicular to the inclination:

$$F_y = \mu mg\cos\theta \tag{12}$$

where m is the calculated mass of the robot, g is the gravitational acceleration, μ is the friction coefficient and θ is the inclination angle of the road. Using Eqs. (11-12), an equation can be derived for the total power requirement to move the robot on the inclined surfaces. The robot's overall power consumption (P_θ) on the inclined surfaces is shown in Eq. (13), where η and V stand for the mechanical transmission efficiency and velocity, respectively:

$$P_\theta = \frac{(mg\sin\theta + \mu mg\cos\theta)V}{\eta} \tag{13}$$

The calculated mass of the robot is 0.952 kg and gravitational acceleration is 9.81 ms^{-2}. The mechanical transmission efficiency and friction coefficient were taken as 0.9 and 0.2, respectively (Hua *et al*., 2016). Thus, the total power requirement was calculated to move the robot on all the inclined surfaces:

$$P_{10^0} = \frac{(0.952kg \times 9.81ms^{-2}\sin 10^0 + 0.2 \times 0.952kg \times 9.81ms^{-2}\cos 10^0)0.028ms^{-1}}{0.9}$$

$$P_{10^0} = 0.107W$$

$$P_{20^0} = 0.0803W$$

$$P_{30^0} = 0.0697W$$

$$P_{40^0} = 0.0637W$$

$$P_{45^0} = 0.0624W$$

$$P_{50^0} = 0.0604W$$

$$P_{60^0} = 0.0571W$$

The startup power requirement with the increased coefficient (K) of 1.5 can be calculated. Additionally, since this design robot has four motors, the power required per motor (P_m) can be calculated using Eq. (14):

$$Pm = \frac{P_\theta \times K}{4} \tag{14}$$

This quarter-car model active suspension system for a mobile robot was put through testing and the outcomes were examined. They are outlined in the results and discussion section.

Results and Discussion

Different angle surfaces were used to evaluate each wheel's formatted active suspension system. The robot's plane constantly attempted to remain horizontal at these angles, as seen in Fig. (8).

In these instances, the screw shaft's height was progressively decreased while traveling up an incline. Similarly, the screw shaft's height was increased gradually as it descended. The robot body maintained horizontal motion in both situations and overcame rolling and bending.

The nut can travel freely and effortlessly along the 10 cm length of the screw because it is 10 cm long. However, at first, the nut is positioned in the center of the screw shaft. Since the nut is positioned in the center of the screw shaft, it can travel in length 5 cm, both up and down. Based on previous calculations, when overcoming an obstacle, the theoretical values of the maximum speed available for driven motors and the maximum distance traveled within 10 sec can be seen in Table (1).

Fig. 8: Testing the robot for different angle surfaces

Table 1: The theoretical values of the maximum speed and distance available for driven motors

The angle of the obstacle	Maximum distance traveled within 10 Sec (cm)	Maximum speed (ms^{-1})
10^0	28.0	0.0280
20^0	14.5	0.0146
30^0	10.0	0.0100
40^0	07.6	0.0077
45^0	07.0	0.0071
50^0	06.5	0.0065
60^0	05.5	0.0057

Table 2: The tested values of the maximum speed for driven motors

	Maximum speed (ms^{-1})	
The angle of the obstacle	Upward	Downward
10^0	0.0255	0.0215
20^0	0.0134	0.0197
30^0	0.0089	0.0073
40^0	0.0071	0.0055
45^0	0.0063	0.0051
50^0	0.0056	0.0049
60^0	0.0053	0.0041

The maximum position of its suspension movement is reached by this mobile robot in 10 sec. Therefore, the robot's maximum length of trip on various angled surfaces was theoretically determined, as shown in the second column. Its length steadily decreased as the angle rose. A similar pattern can be seen in the maximum speed that driven motors can achieve. Subsequently, the mobile robot was tested on various angled surfaces to obtain the results. Here, the maximum speed that driven motors were obtained for the same angle when the robot was moving up and down. The results can be seen in Table (2).

The observed measurements show that the tested and theoretical values differ slightly. There could be several causes, including surface or road friction, environmental conditions, measurement noises, and instrument inaccuracies. Nonetheless, the maximum speed of driven motors steadily decreases when the angle of the space is higher. For this robot, it is necessary to keep the wheel-driven motor speed lower than the above-tested values. The robot would not be able to remain horizontal when it passes an obstruction if it could not maintain values below these.

For various terrain conditions, the responses from the gyro and accelerometer sensors were examined. Both obstacle identification and wheel speed adjustment based on acquired data were aided by it. In this section, the graphical representation of the accelerometer and gyro responses has been outlined.

As the vehicle moves over a flat surface, the accelerometer and gyro sensor responses are shown in the graph depicted in Fig. (9). According to that, there is no obstacle present and the terrain can be determined to be level and smooth.

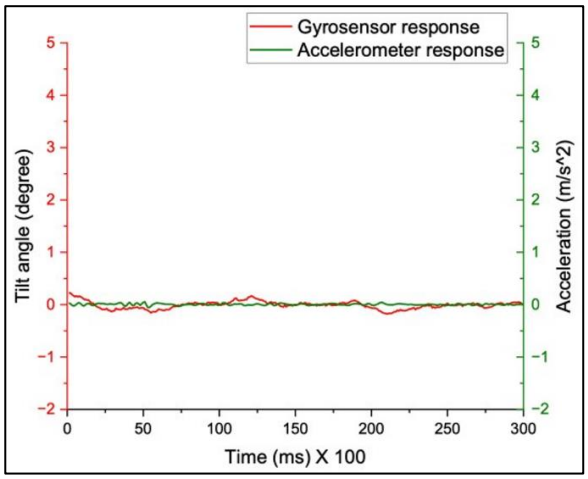

Fig. 9: Graph of the accelerometer and gyro sensor responses in plain terrain

The sensor detects a change in the angle of the sensor and the gyro sensor detects the upward acceleration in Fig (10). So, the system can identify the situation and position can be recovered by changing the height of the corresponding linear actuator. The accelerometer response shows that the recovery tie is much higher. So, the rover should reduce the speed and this is where the system can identify whether the speed of the motor should be increased or decreased.

The gyro sensor occasionally produces upward accelerations and the accelerometer response continuously displays the increment of the sensor angle in Fig. (11). According to the sensor outputs, the rover does not maintain its initial position and continuously tilts. The response of the linear actuator is not enough to recover the rover position due to the limitations of the actuator. The wheel's speed should be decreased up to a particular amount to handle this scenario. The sensor outputs are monitored by the system continuously and decides to reduce speed due to continuous tilting. The process is done by analyzing sensor responses at a fixed time interval. The system can identify whether the sensor angle is recovered or not and reduce the speed by 30% of its current speed.

When an obstacle is detected, the gyro sensor response will provide a change in the angle of the sensor and if it appears, as shown in Fig. (12), the rover will recognize it as an obstacle that needs to be pushed up. The gyro sensor gives an upward acceleration and the system can reduce the height of the corresponding actuator of the rover.

The graph in Fig. (13). shows the reduction in speed and quick recovery of the angle. The reduced speed is 30% of the current speed in every 500 ms time slot and the system understands the speed is higher. The best approach is to reduce the speed by 30-40% of its speed to get the best performance with the speed of the linear actuator (Gamage *et al*., 2024).

DOI: 10.3844/jmrsp.2024.39.48

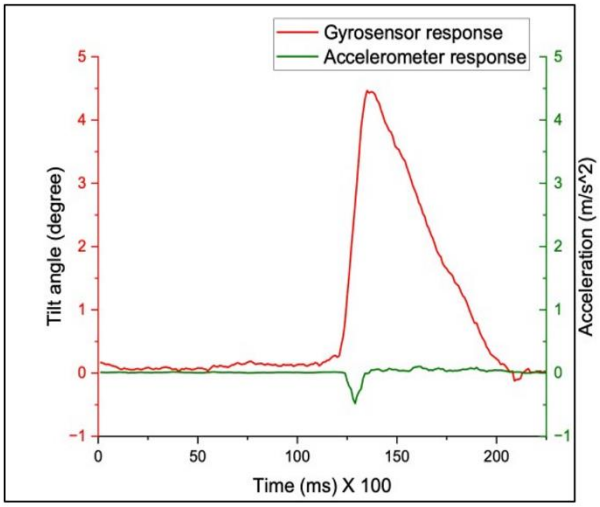

Fig. 10: Graph of the obstacle detection and recovery position

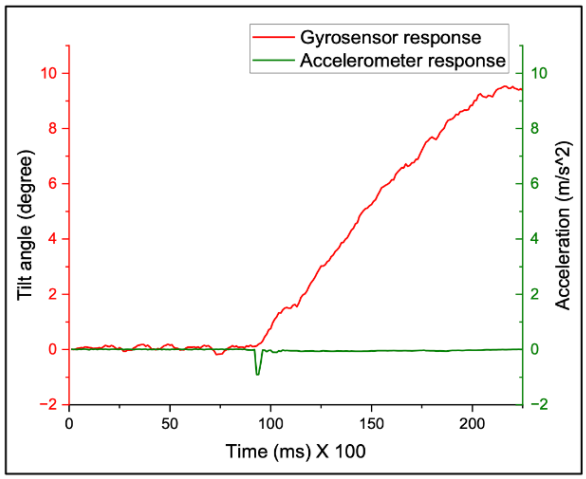

Fig. 11: Graph of the obstacle detection and unrecovered

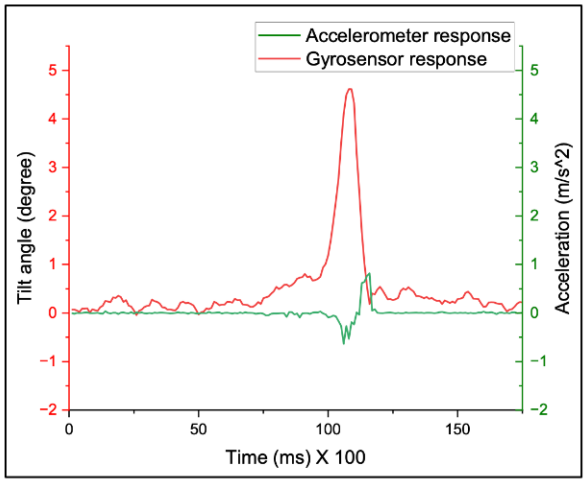

Fig. 12: Graph of the small obstacle detection

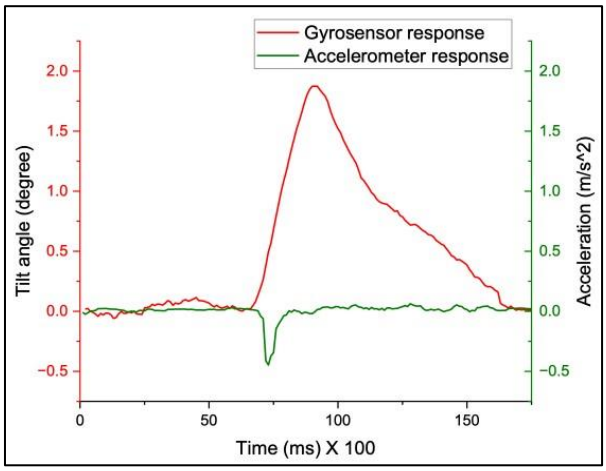

Fig. 13: Graph of the recovering position by reducing the speed

Conclusion

- This project aims to design and develop an active suspension system for a mobile robot, which would help robots move forward, overcome obstacles, and increase stability as well as mobility
- The suspension system was designed and developed from the quarter-vehicle model to a four-wheel robot with an active suspension system
- Various angled surfaces were used to evaluate the robot's modeled active suspension system
- Its unique feature is its constant effort to stay horizontal and overcome rolling and bending
- Furthermore, introducing this novel solution can address important problems, including the control systems' intricacy, the production cost increase, and the complex structure of the existing robot suspension system

Acknowledgment

This research's success is especially due to the academic and non-academic staff of the Technology Faculties of Colombo and Uva Wellassa Universities in Sri Lanka.

Funding Information

The authors have not received any financial support or funding to report.

Author's Contributions

Rukshan Gamage: Contributed to the conceptualization, design, curation, and analysis of data.

Chamod Rathnayake: Contributed to the writing of the original draft, design, formal analysis, and conceptualization of this study.

Ruwan Kalubowila: Contributed to the acquisition of data, supervision, and investigation.

Sanjaya Thilakarathne: Contributed to the supervision, investigation and visualization of the study.

Ethics

This article is unique and contains content that hasn't been published before. This original article has been reviewed and approved by all co-authors, and the corresponding author attests that there are no ethical issues. Additionally, the authors declare that they have no conflicts of interest in this study.

References

Attia, T. S. A. (2018). *Design and Development of a Novel Reconfigurable Wheeled Robot for Off-Road Applications*. Virginia Tech.

Badrinarayanan, S., Kumar, V. R., Bhinder, K. S., & Ralexander. (2018). Electro mechanical linear actuator using roller screws. *IOP Conference Series: Materials Science and Engineering*, *402*(1), 012101. https://doi.org/10.1088/1757-899x/402/1/012101

Bledt, G., Powell, M. J., Katz, B., Di Carlo, J., Wensing, P. M., & Kim, S. (2018). MIT Cheetah 3: Design and Control of a Robust, Dynamic Quadruped Robot. *2018 IEEE/RSJ International Conference on Intelligent Robots and Systems (IROS)*, 2245–2252. https://doi.org/10.1109/iros.2018.8593885

Bluethmann, B., Herrera, E., Hulse, A., Figuered, J., Junkin, L., Markee, M., & Ambrose, R. O. (2010). American Institute of Aeronautics and Astronautics, & IEEE Aerospace and Electronic Systems Society. *2010 IEEE Aerospace Conference*, 1–9. https://doi.org/10.1109/AERO.2010.5446895

Chetan, R. G., Both-Rusu, R., Dulf, E.-H., & Festila, C. (2017). Physical model of a quarter-car active suspension system. *2017 18th International Carpathian Control Conference (ICCC)*, 517–520. https://doi.org/10.1109/carpathiancc.2017.7970455

Cloutier, J. (2014). *Simulation and Control of a Ball Screw System Actuated by a Stepper Motor with Feedback*. University of Guelph.

Crenganis, M., Biris, C., & Girjob, C. (2021). Mechatronic Design of a Four-Wheel drive mobile robot and differential steering. *MATEC Web of Conferences*, *343*, 08003. https://doi.org/10.1051/matecconf/202134308003

Datar, A., Pan, C., Nazeri, M., & Xiao, X. (2024). Toward Wheeled Mobility on Vertically Challenging Terrain: Platforms, Datasets, and Algorithms. *2024 IEEE International Conference on Robotics and Automation (ICRA)*, 16322–16329. https://doi.org/10.1109/icra57147.2024.10610079

Dave, D., Pipaliya, S. B., Pipaliya, B. B., & Koradiya, P. (2014). Design Development& Investigation of Remote Controlled Screw Jack for Four Wheelers cars. *Technix International Journal for Engineering Research*, *1*(6), 25–30.

Dogruer, C. U. (2019). Improving Ride-Comfort of a Quarter-Car Model using Modal Control. *2019 7th International Conference on Control, Mechatronics and Automation (ICCMA)*, 237–242. https://doi.org/10.1109/iccma46720.2019.8988621

Elfasakhany, A., Yanez, E., Baylon, K., & Salgado, R. (2011). Design and Development of a Competitive Low-Cost Robot Arm with Four Degrees of Freedom. *Modern Mechanical Engineering*, *01*(02), 47–55. https://doi.org/10.4236/mme.2011.12007

Fotuhi, M. J., Karaman, C., & Bingül, Z. (2022). Design and development of a ball-screw and electrical motor driven industrial electromechanical cylinder. *Sigma Journal of Engineering and Natural Sciences*, *40*(4), 822–830. https://doi.org/10.14744/sigma.2022.00098

Gamage, R., Rathnayake, C., Kalubowila, K. D. R. N., & Thilakarathne, S. (2024). Development of a Real-time Terrain Adaptation and Navigation Robot with Independent Height Adjustment of Struts and Wheel Speed Optimization. *8th International Research Conference of Uva Wellassa University, IRCUWU2024*, 128.

Hua, F., Li, G., Liu, F., & Liu, Y. (2016). Mechanical design of a four-wheel independent drive and steering mobile robot platform. *2016 IEEE 11th Conference on Industrial Electronics and Applications (ICIEA)*, 235–238. https://doi.org/10.1109/iciea.2016.7603585

Jinasena, K. K., & Meegama, R. G. N. (2016). Design of a Low-cost Autonomous Mobile Robot. *International Journal of Robotics and Automation (IJRA)*, *2*(1), 113–125.

Li, L., Jiang, S., Dai, F., & Gao, X. (2014). Dynamic model and balance control of two-wheeled robot with non-holonomic constraints. *Proceeding of the 11th World Congress on Intelligent Control and Automation*, 503–508. https://doi.org/10.1109/wcica.2014.7052764

Mallikarathne, T., Rathnayake, C., Abeysinghe, H., & Perera, M. (2023). Design a Beach Cleaning Robot Based on AI and Node-RED Interface for Debris Sorting and Monitor the Parameters. *2023 7th SLAAI International Conference on Artificial Intelligence (SLAAI-ICAI)*, 1–6. https://doi.org/10.1109/slaai-icai59257.2023.10365015

Ni, L., Ma, F., & Wu, L. (2020). Posture Control of a Four-Wheel-Legged Robot with a Suspension System. *IEEE Access*, *8*, 152790–152804. https://doi.org/10.1109/access.2020.3017662

Oftadeh, R., Aref, M. M., Ghabcheloo, R., & Mattila, J. (2013). Mechatronic Design of a Four Wheel Steering Mobile Robot with Fault-Tolerant Odometry Feedback. *IFAC Proceedings Volumes*, *46*(5), 663–669. https://doi.org/10.3182/20130410-3-cn-2034.00092

Olinski, M., & Cholewa, K. (2014). Design and simulation of a mobile platform with a semi-active suspension for uneven terrain. *Journal of Theoretical and Applied Mechanics*, *62*(2), 279–292. https://doi.org/10.15632/jtam-pl/184231

Pan, Z., Li, B., Jing, H., Niu, Z., & Wang, R. (2023). Wheel-Leg Collaborative Control for Wheel-legged Robots Based on MPC with Preview. *2023 IEEE International Automated Vehicle Validation Conference (IAVVC)*, 1–8. https://doi.org/10.1109/iavvc57316.2023.10328121

Pei, Y., & Kleeman, L. (2016). Mobile robot floor classification using motor current and accelerometer measurements. *2016 IEEE 14th International Workshop on Advanced Motion Control (AMC)*, 545–552. https://doi.org/10.1109/amc.2016.7496407

Romsai, W., & Nawikavatan, A. (2019). Optimal PIDA Controller Design for Quarter Car Suspension System by Intensified Current Search. *2019 17th International Conference on ICT and Knowledge Engineering (ICT&KE)*, 1–5. https://doi.org/10.1109/ictke47035.2019.8966863

Sucuoğlu, H. S., Bogrekcı, I., Demırcıoglu, P., & Turhanlar, O. (2016). Analysis of Suspension System for 3D Printed Mobile Robot. *International Journal of Applied Mathematics, Electronics and Computers*, *Special Issue*, 329–329. https://doi.org/10.18100/ijamec.270660

Sujiwa, A., & Suhadata. (2023). Design and Construction of a Self-Balancing Robot using Long Range Control Based on NRF24L01. *BEST : Journal of Applied Electrical, Science, & Technology*, *5*(2), 34–37. https://doi.org/10.36456/best.vol5.no2.8165

Unluturk, A., & Aydogdu, O. (2017). Adaptive control of two-wheeled mobile balance robot capable to adapt different surfaces using a novel artificial neural network–based real-time switching dynamic controller. *International Journal of Advanced Robotic Systems*, *14*(2). https://doi.org/10.1177/1729881417700893

Yildiz, A. S., Sivrioglu, S., Zergeroglu, E., & Cetin, S. (2013). Adaptive control of semiactive quarter car model with MR damper. *2013 9th Asian Control Conference (ASCC)*, 1–6. https://doi.org/10.1109/ascc.2013.6606324

Zheng, J., Gao, H., Yuan, B., Liu, Z., Yu, H., Ding, L., & Deng, Z. (2018). Design and terramechanics analysis of a Mars rover utilising active suspension. *Mechanism and Machine Theory*, *128*, 125–149. https://doi.org/10.1016/j.mechmachtheory.2018.05.002

Zunaidi, I., Kato, N., Nomura, Y., & Matsui, H. (2006). Positioning System for 4Wheel Mobile Robot: Encoder, Gyro and Accelerometer Data Fusion with Error Model Method. *CMU. Journal*, *5*(1), 1–14.